Indian Journal of Experimental Biology
Vol. 63, December 2025, pp. 980-992
DOI: 10.56042/ijeb.v63i12.19365

Mechanistic insights into diesel exhaust-induced lung cancer cell survival through AhR signaling

Ankita Bagde[1,2], Atul Katarkar[1], B Srimuruganandam[3]& K Krishnamurthi[1,2]*

[1]Environmental Health and Toxicology, CSIR-National Environmental Engineering Research Institute, Nagpur 440020, Maharashtra, India

[2]Academy of Scientific and Innovative Research, Ghaziabad-201002, Uttar Pradesh, India

[3]Centre for Clean Environment, Vellore Institute of Technology, Vellore 632014, Tamil Nadu, India

Received 02 May 2025; revised 24 September 2025

Diesel exhaust (DE), a Group I human carcinogen, is a major environmental pollutant that significantly contributes to global lung cancer burden. Nitro-polycyclic aromatic hydrocarbons (PAHs), particularly 1-nitropyrene (1NP) and its metabolite 1-aminopyrene (1AP), are key markers of DE exposure. Although DE has been strongly linked to genomic instability, the molecular mechanism underlying this process remains poorly understood, especially the role of aryl hydrocarbon receptor (AhR) in promoting lung cancer cell survival and carcinogenesis. To address this gap, we examined the effect of 1NP/1AP in A549 cells. Exposure to 1NP/1AP significantly induced reactive oxygen species (ROS, $P<0.01$) and DNA damage ($P<0.0001$, as evaluated using Dichloro-dihydro-fluorescein diacetate and the comet assay, respectively. AhR activation was confirmed by AhR nuclear translocation (immunofluorescence, $P<0.0001$) and *CYP*-gene expression by qRT-PCR analysis ($P<0.0001$). Despite such genomic instability, A549 cells continued to exhibit colony formation, migration, and spheroid growth, which were not significantly altered. Conversely, inhibition of AhR activity enhanced apoptosis ($P<0.0001$), and markedly reduced cell migration, colony formation, and spheroid growth ($P<0.001$). Furthermore, an increased γ-H2AX expression was positively correlated with DNA damage ($P<0.001$), suggesting that AhR activation may regulate DNA damage repair and facilitate the survival of A549 cells under 1NP/1AP insult. Our findings highlight the previously unexplored role of AhR in promoting DNA repair and lung cancer cell survival and suggest that AhR inhibition may serve as a promising therapeutic strategy for preventing DE-induced lung carcinogenesis.

Keywords: Lung cancer, AhR, 1-nitropyrene, 1-aminopyrene, Genomic instability, DNA damage

Lung cancer (LC) is the second leading cause of cancer-related mortality. 2.48 million new cases of lung cancer were diagnosed worldwide in 2022[1]. An often-overlooked risk factor for LC is ambient air pollution. Recently, the exposure to particulate matter (PM ≤2.5 μm or $PM_{2.5}$) in the environment has been closely linked to LC[2]. $PM_{2.5}$ can pass into the lower respiratory tract, reach the alveoli, and may enter the systemic circulation[3]. Diesel particulate matter (DPM) is a key component of DE. It has a diameter of <1 μM and is categorised as human carcinogenic (Group 1)[4]. 1NP, a key polycyclic aromatic hydrocarbon (PAH) and a potential surrogate marker for diesel particulate matter (DPM), is classified as a Group 2A carcinogen and plays a substantial role in carcinogenic and mutagenic effects. Long-term exposure to animals (>12 weeks) shows the accumulation of 1NP in the lung, liver, and mammary gland. Recent studies have demonstrated its carcinogenic effect on LC metastasis in both *in vitro* and *in vivo*[5]. Till now, the cancer-causing effects of 1NP have been curiously studied in terms of cellular stress due to free radicals, DNA adducts formation, and deregulation of key cellular pathways[6].

PAHs that enter lung cells are considered pro-carcinogens since they cannot interact with DNA directly[7]. Rather, it is their conversion into carcinogenic metabolites that contributes to cancer development[8]. 1NP generates ROS and induces DNA oxidative lesions, contributing to mutagenicity and genotoxicity. However, the mutagenic pathway is complex and driven by several metabolite activations through nitro-reduction and the sequential formation of 1-nitrostyrene, N-hydroxyl-1AP, and 1AP. A recent study has further highlighted the conversion of 1NP to 1AP in A549 cells[9]. This is certainly a crucial finding relevant to examining the direct impact of 1AP on the development of lung carcinogenesis, as DE directly exposes lung tissue.

*Correspondence:
Phone: +91 712 2249757
E-mail: krishnamurthi.k@csir.res.in:
krishnamurthikannan@gmail.com

Aryl hydrocarbon receptor (AhR) is well-recognised for its role in detecting and responding to environmental chemicals, particularly PAHs[10]. Upon ligand binding, AhR translocate to the nucleus and dimerises with the AhR nuclear translocator (ARNT), activating target genes such as cytochrome P450 (*CYP*) enzymes[11,12]. This pathway has been implicated in several biological processes, including inflammation, cellular proliferation, tumorigenesis, and metastasis. However, its role in genomic instability, a critical hallmark of tumor development, remains poorly defined. In this study, we investigated the contribution of AhR in DNA repair mechanisms and cell survival following exposure to genotoxic 1-nitropyrene (1NP) and 1-aminopyrene (1AP). Using A549 human lung carcinoma cells as a model, we examine the effects of AhR inhibition on cell survival, DNA damage response, and tumorigenic properties such as 3D spheroid growth, migration, and colony formation. Our findings suggest that AhR activation is crucial in mediating DNA repair and promoting cell survival under genotoxic stress. Taken together, this study highlights AhR as a potential therapeutic target for mitigating environmental DNA damage and preventing LC progression exposed to DE.

Materials and Methods

Chemicals and reagents

The standards of 1NP (5522-43-0), 1AP (1606-67-3), and N-acetyl-L-cysteine (100098, NAC) were procured from Sigma-Aldrich. Dimethyl sulfoxide (MB186-1G, DMSO) was from Fisher Scientific. 3-(4,5-dimethylthiazol-2-yl)-2,5-diphenyltetrazolium bromide (1042120, MTT) and Dichloro-dihydro-fluorescein diacetate (DCFH-DA, RM349-10G) from Hi-media. Ham's F12-modified cell culture medium with L-glutamine without sodium bicarbonate was obtained from MP Biomedicals. Other reagents, fetal bovine serum (FBS) and antibiotic-antimycotic (100X, A002-50 mL), were obtained from Gibco. AhR monoclonal antibody (primary antibody, MA1-513) and Alexa-Fluor 555 (secondary antibody, A31570) were purchased from Thermo-Fischer, while the AhR antagonist (182705-10G) was from Merck. Matrigel (354277) was procured from Corning. Double de-ionised (DI) water was used for all the experiments to avoid contamination and hindrance. Other required chemicals were obtained from commercial sources.

Cell culture and chemical treatment

A549 (Human adenocarcinoma epithelial cells) were procured from NCCS Pune (India) and grown in suitable condition media containing 10% FBS at 37°C with a 5% CO_2 incubator. A 1NP and 1AP stock solution in DMSO was prepared. The cells were exposed to 1NP and 1AP, either with or without pre-treatment of NAC (1 mM) or AhR inhibitor (10 µM), to achieve the desired final concentrations for subsequent experiments. Control in the experiment was achieved by treating A549 cells with DMSO.

Cell viability test by MTT assay

MTT assay on A549 cells with exposure to different concentrations of 1NP/1AP was performed as per the protocol described by Kumar *et al*.[13]

Alkaline comet assay

The comet test was used to examine the DNA damage, as described in the protocol earlier Olive PL & Banáth[14] JP and Katarkar *et al.*[15] Briefly, 4×10^5 A549 cells/well were plated in a transparent 6-well cell culture plate and exposed to 1NP (2 µM and 5 µM) and 1AP (350 nM and 900 nM), along with or without NAC (1 mM) and AhR inhibitor (10 µM) for 24 hours. Standard melting agarose (1%) was used to coat the slides and allow them to dry. After the exposure, the cells were harvested and suspended in 0.2 mL 1X PBS. The suspended cells were mixed with 0.5% low-melting agarose and placed on the agarose-coated slides. The slides were then kept on the ice to solidify for 1 hour. They were then kept in lysis buffer (pH 10) at 4°C for 2 hours, followed by incubations in an alkaline solution (pH>13) to unwind the DNA strands and run for electrophoresis at 25 V for 20 min. The slides were stained with EtBr. Stained slides were visualized using an Olympus BX51 fluorescent microscope (U-LH100 HG made in Japan) at 40X magnification. The slides were analyzed. All 50 images were taken for each slide, and DNA damage was quantified in % tail DNA by Comet score software.

ROS generation and NAC scavenging activity

The intracellular ROS generation and NAC scavenging effect were measured by DCFH-DA assay[16,17]. A549 cells were seeded on a glass coverslip placed inside six-well plates and exposed to the 1NP/1AP with and without 1 mM NAC for 24 hours. After that, they were treated with DCFH-DA (10 µM) for 20 min at 37°C. The cover slip was washed with 1X PBS and mounted on glass slides. Fluorescent

images were captured by an Olympus BX51 fluorescence microscope.

Colony assay

A colony assay was conducted using crystal violet staining to assess cell proliferation[18]. 6-well plates were seeded with 1×10^3 A549 cells. The cells were treated with 1NP and 1AP with or without NAC for seven days. After seven days, the media was removed from the cells and replaced with fixative 4% paraformaldehyde for 10 min. Colonies were stained using 0.05% crystal violet for 60 min, and the plates were gently washed with tap water to remove any leftover stains and dried further. After that, the quantity of colonies for every condition was determined.

Immunofluorescence assay

An immunofluorescence assay was performed to detect the AhR localization. A549 cells were seeded on coverslips and treated with 1NP/1AP for 24 hours. Sequentially, cells were fixed (4% formaldehyde) for 10 min, permeabilized (1% Triton X-100) for 20 min, and blocked (1% BSA) for 120 min. AhR-specific primary antibody incubation was performed overnight at 4°C. After the coverslip was rinsed with 1X PBS, it was further incubated with Alexa Fluor 594-conjugated secondary antibodies for 120 min. After additional PBS washes, cell nuclei were counter-stained with DAPI and mounted. Slides were visualized using an Olympus BX51 fluorescence microscope.

RNA extraction and quantitative reverse-transcription polymerase chain reaction (qRT-PCR)

About 4×10^5 A549 cells/well were plated for gene expression analysis. The cells were exposed to 1NP and 1AP, either with or without an AhR inhibitor (10 μM), for another 24 hours. Total RNA was isolated using the TriZol reagent method[19]. Quantification and purity of RNA were assessed using a nanodrop (DeNovix) at a 260/280 nm ratio. Complementary DNA (cDNA) was prepared using reverse transcriptase enzyme and random primer. For qRT-PCR analysis, cDNA was used with specific oligonucleotide primers for *CYP1A1, CYP1A2*, and *β-actin*[20]. Gene expression was analysed per the manufacturer's protocols using a Power SYBR Green PCR master mix. CT value was determined (Applied Biosystem, Quant Studio 3). Relative mRNA expression of genes was compared and normalised against the β-actin gene. Gene expression profiles were then generated using GraphPad Prism software.

Annexin V/ DAPI apoptosis assay

Annexin V and DAPI were used in apoptosis experiments[21]. A549 (5×10^5 cells/well) were seeded on a coverslip. The cells were exposed to 1NP/1AP for 24 hours, either with or without an AhR inhibitor. Cells were then rinsed with 1X PBS, followed by 1X binding buffer (10 min), and washed with 1X PBS. Finally, cells were incubated with 0.25 μg/mL Annexin V solution (prepared in 1X binding buffer) in the dark for 10 to 15 min. The percentage of apoptotic cells for each condition was then determined once the slides were ready for fluorescence microscopic examination.

Scratch assay

Cell migration was performed by using the scratch assay[22]. Briefly, 5×10^5 cells/well A549 cells were seeded in 6-well plates. Once the cells achieved 80% confluency, the scratch was made using a 20 μL sterile tip and then washed with 1-X PBS. Scratched cells were then photographed for 0 h, followed by the treatment of 1NP or 1AP with and without AhR for the next 24 hours. Cell migration was expressed as a percentage scratch closing area.

3D culture assay

A 3D culture assay was used to assess the formation of the spheroid[23]. Matrigel was thawed on ice, and 10% of the Matrigel solution was prepared. A 200 μL aliquot of the mixture was then placed on 8-chambered glass slides and incubated at 37°C for 30 min**.** Five hundred cells were resuspended in a 2% Matrigel solution prepared in media. Finally, each well was filled with 200 μL of the cell-Matrigel mixture and incubated for 16 hours. Treatment of 1NP and 1AP, both with and without AhR inhibitor, was cultured for 8 days and observed under a microscope for spheroid formation. Spheroid size as a diameter was calculated using the ImageJ software[24].

Statistical analysis

GraphPad Prism software 8.0 and MS Excel were used for calculation and statistical analysis. Data were represented as mean ± standard deviation (SD). The student's *t*-test (two-tailed, unpaired) was used for data analysis to compare the means of the two groups. All the experiments were performed in triplicate (n=3). *P*-value < 0.05 was considered statistically significant.

Results

1NP-induced genomic instability in A549

A549 cells were exposed to 1NP ranging from 25 µM to 200 µM for 24 hours, and the LC50 value was determined to be 101.2 µM (Fig. 1A). For subsequent experiments, to explore 1NP toxicity, sub-cytotoxic doses of 1NP corresponding to 1/50th (≈ 2 µM) and 1/20th (≈ 5 µM) of the LC50 were selected. 1NP-induced genotoxicity was evaluated by the comet assay. The results showed 1NP induced dose-dependent increase in DNA damage (P<0.0001) compared to control (DMSO treated), as shown in (Fig. 1B). To investigate whether ROS induced DNA damage, we assessed intracellular ROS production using the DCFH-DA immunofluorescence imaging protocol, both with and without antioxidant NAC treatment. As shown in (Fig. 1C), a markedly increased ROS level was observed in 1NP-treated A549 cells compared to the DMSO control, while co-treatment with NAC suppressed ROS in cells treated with 1NP + NAC (P<0.0001). Consistently, comet assay analysis showed a significant reduction in DNA damage in the 1NP + NAC-treated compared to the 1NP-treated cells alone (Fig. 1D).Together, these results suggested that 1NP induces DNA damage in A549 cells mediated by ROS and contributing to 1NP-induced genotoxicity.

1AP genotoxicity in A549 cells

1NP metabolites have been suggested as a more reliable indicator of DPM exposure. 1NP is partially metabolised to 1AP, which is known to generate DNA adducts. Therefore, we explore the genotoxic effect of 1AP in A549 cells, cytotoxicity analysis using MTT assay with concentrations ranging from 10 µM to 50 µM for 24 hours. The LC50 value was calculated and observed to be 17.86 µM, as shown in (Fig. 2A). Likely, 1/20th (~900 nM) and 1/50th (~350 nM) dose of 1AP were selected for further experiments. DNA damage was then assessed by comet assay, which showed a dose-dependent DNA damage in 1AP-treated A549 cells (P<0.0001) compared to control (Fig. 2B). To examine whether this genotoxicity was mediated by ROS, DCFH-DA assay was used to measure the intracellular ROS. As indicated in (Fig. 2C), a significant elevation of intracellular ROS was detected in 1AP-treated cells (P<0.0001)

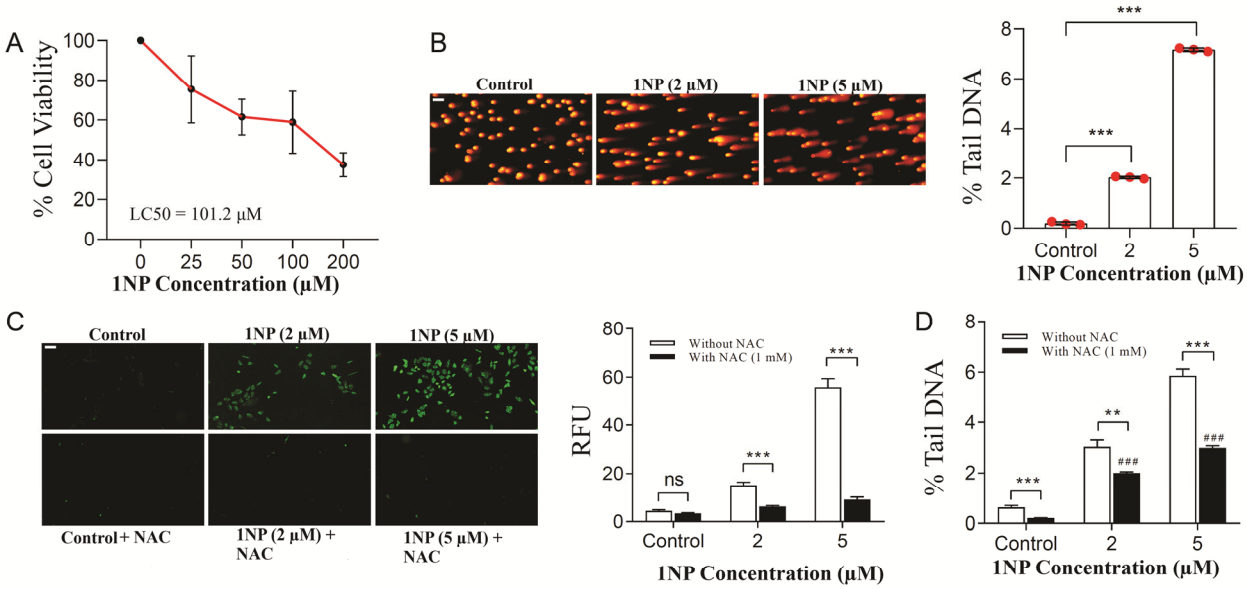

Fig. 1 — Effects of 1-nitropyrene (1NP) on cell viability, ROS generation, and DNA damage in A549 cells. (A) Cell viability of A549 cells following 24 h exposure to 1NP, evaluated using the MTT assay. Dose-dependent cell viability demonstrating cytotoxic potential of 1NP (B) DNA damage induced by 1NP in A549 cells, left: representative comet images showing increased tail length in 1NP-treated cells compared to controls. Right: quantification of DNA damage, expressed as % tail length, with >50 cells analysed per sample. (C) Intracellular ROS production in A549 cells exposed to 1NP with or without the antioxidant NAC, 1 mM. Left: representative fluorescence images (green signal indicates ROS). Right: quantification of relative fluorescence units (RFU) showing that NAC significantly attenuated 1NP-induced ROS enrichment. (D) DNA damage analysis of A549 cells treated with 1NP in the presence or absence of NAC, revealed that NAC co-treatment reduced 1NP-induced DNA strand breaks. >50 cells were analysed per sample. [Data expressed as mean ± SD. ns = non-significant, **P < 0.001, *** or $^{###}P$ < 0.0001. Scale bar: 20 µm. (n = 3)]

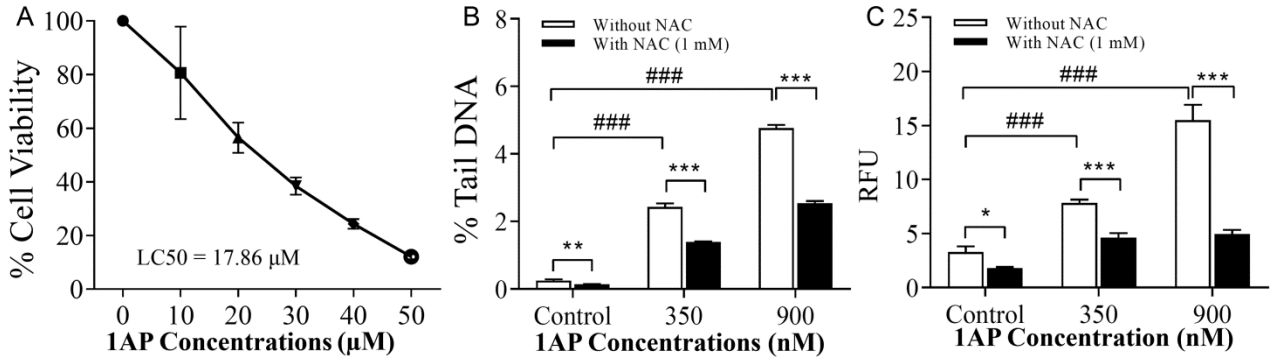

Fig. 2 — Effects of 1AP on cell viability, ROS generation, and DNA damage in A549 cells. (A) Cell viability of A549 cells after 24 h exposure to 1AP, indicating the cytotoxic potential of 1AP. (B) Quantification of DNA damage in A549 cells treated with 1AP in the presence or absence of NAC. DNA strand breaks were analysed in >50 cells per sample. NAC treatment markedly reduced 1AP-induced DNA damage. (C) Intracellular ROS levels in A549 cells exposed to 1AP with or without NAC. >50 cells analysed per sample, showing that NAC significantly attenuated 1AP-induced ROS enrichment. [Data are expressed as mean ± SD. * P< 0.05, ** P < 0.001, *** or ### P < 0.0001; ns = non-significant. SD = standard deviation. (n=3)]

compared to DMSO-treated control cells. In contrast, cells treated with 1AP+NAC exhibited a ROS scavenging effect. Reduction in DNA damage was detected in cells exposed to 1AP + NAC, compared to those treated with 1AP alone. These results indicate that the ROS scavenging effect alleviates DNA damage.

Colony formation unaffected by 1NP/1AP exposure

To assess whether ROS generation and DNA damage affect the long-term cell proliferation of A549 cells, a colony formation assay was conducted with both the compounds (1NP and 1AP) with and without NAC. According to our previous results, despite ROS generation and genotoxic effect, 1-NP-treated cells exhibited dense colony formation and did not significantly alter the number of colonies compared to control, and co-treatment with NAC indicates no additional effect, as shown in (Fig. 3A). A Similar pattern was observed in 1AP-exposed cells. As depicted in (Fig. 3B), colony formation remained unaffected, irrespective of NAC co-treatment.

1NP/1AP exposure-induced AhR activation

AhR facilitates cancer cell proliferation, invasion, migration, and survival, even in the absence of environmental toxins[25–27]. However, under environmental exposure, the contribution of AhR in the survival of A549 cells and carcinogenesis is highly elusive. Hence, the present study evaluated the activation of AhR in the context of A549 cells in relation to its cellular localisation. Immunofluorescence images analysis revealed nuclear translocation of AhR (red) and nuclei (DAPI, blue) in cells treated with 1NP/1AP, with or without a specific AhR inhibitor, as shown in (Fig. 4A) using AhR-specific antibody. A pronounced nuclear translocation of AhR was observed (pink in merged images, indicated by arrows) compared to the control, which exhibited predominantly cytoplasmic AhR. Inhibition of AhR effectively prevented this nuclear translocation. Quantification data presented in (Fig. 4B)demonstrated a significant increase in nuclear AhR localisation in 1NP/1AP-treated (P<0.001) compared to control, while co-treatment with AhR inhibitor markedly reduced nuclear AhR level. Increased mRNA expression of AhR target genes, *CYP1A1* and *CYP1A2*, further confirmed the AhR activation. Both genes were significantly upregulated in response to 1NP/1AP treatment (P<0.0001). Meanwhile, AhR inhibition reduced the expression of *CYP1A1* and *CYP1A2*, confirming the specificity of AhR-mediated transcriptional regulation (Fig. 4C). To establish AhR activation, an AhR inhibitor was used as a specific effect. Simultaneous treatment of AhR inhibitor with 1NP/1AP dramatically suppressed nuclear translocation of AhR protein and mRNA expression of *CYP1A1* and *CYP1A2* genes.

Effect of AhR inhibitor on genotoxicity, colony formation, and apoptosis in 1NP/1AP exposed A549 cells

We simultaneously exposed A549 cells to 1NP/1AP, with or without an AhR inhibitor. To evaluate the role of AhR in regulating genotoxic stress responses. Genotoxicity was further assessed with the DNA double-strand break marker phospho-gamma-H2AX (Ser139) by immunofluorescence and comet assay. Interestingly, co-treatment of A549 cells

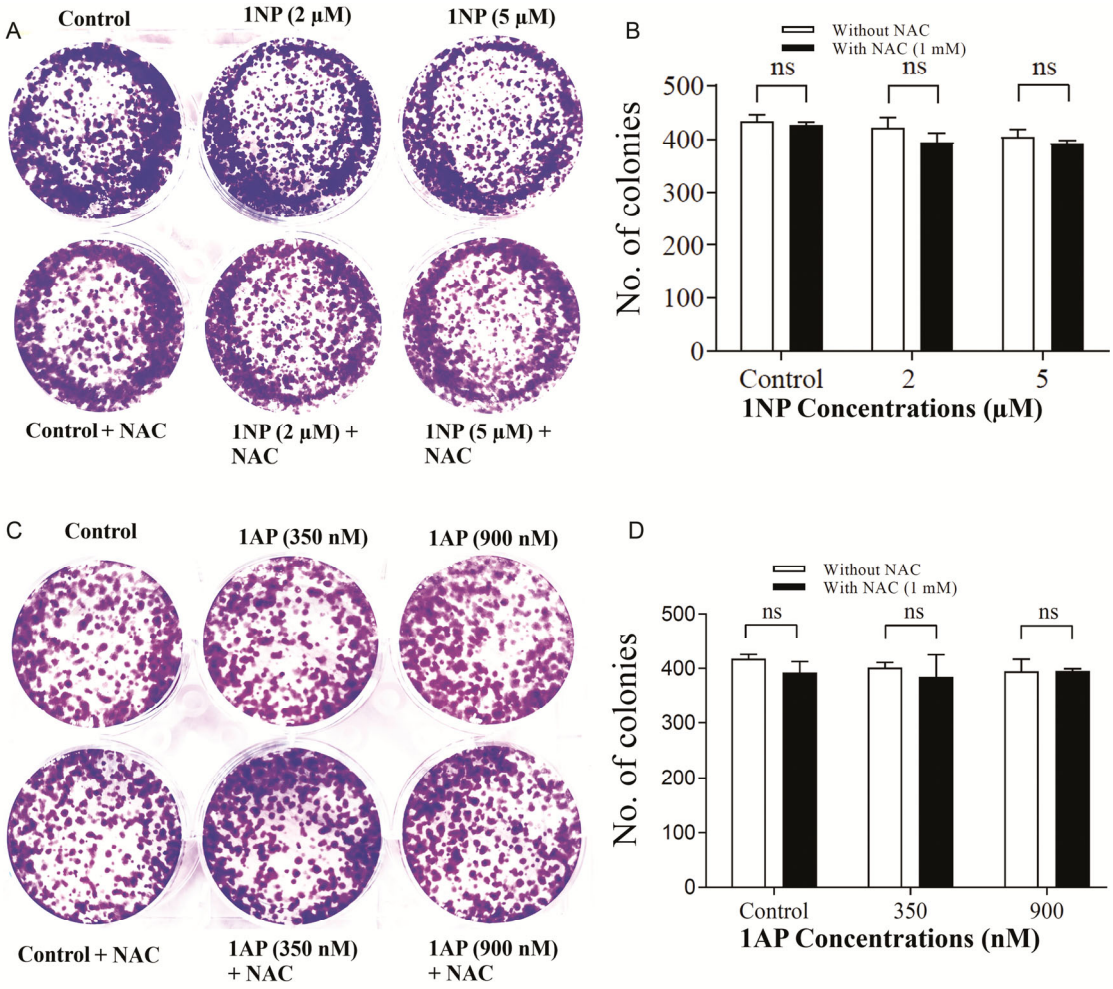

Fig. 3 — Effect of 1NP and 1AP on clonogenic potential of A549 cells. (A &C) Representative images (left) and (B & D) quantification (right) of colony formation assays performed in A549 cells treated with (A) 1NP and (C) 1AP, with or without NAC. After 7 days of incubation, colonies were stained and counted. No significant differences in colony-forming ability were observed across treatments (n = 3). [Data are expressed as mean ± SD. non-significant changes (ns). SD = standard deviation]

with 1NP/1AP and an AhR inhibitor resulted in a markedly higher number of gamma-H2AX foci (P<0.0001) compared to cells treated with 1NP/1AP alone, as shown by immunofluorescence images, and further supported by quantification of foci per cell depicted in (Fig. 5A & B). Moreover, comet assay analysis showed that A549 cells treated with 1NP/1AP, in combination with an AhR inhibitor, exhibited significantly higher % tail DNA than cells treated with 1NP/1AP alone (Fig. 5C& D). This suggested that AhR might play a significant role in the DNA repair mechanism. A colony assay was performed to understand its effect on proliferation. Likely, a reduction in colony formation capability was observed in AhR inhibitor-treated A549 cells compared to 1NP/1AP-treated cells alone (Fig. 5D & E). These results demonstrate that inhibition of AhR exacerbates DNA double-strand breaks and reduces the proliferative capacity of A549 cells. However, the reduction in colony formation was correlated with significantly higher levels of apoptosis in AhR inhibitor-treated A549 cells compared to those treated with 1NP/1AP alone. These observations were further supported by immunofluorescence imaging and quantification of apoptotic cells in (Fig. 6A & B). These findings confirm that AhR activation confers a survival advantage to A549 cells, enabling them to withstand the genotoxic stress induced by 1NP/1AP.

Effect of AhR inhibitor on migration and 3D sphere formation in 1NP and 1AP treated A549 cells

The effects of 1NP/1AP exposure on the migration of A549 cells were evaluated by using the scratch assay. As shown in Fig. 7A & B**,** scratch closure was enhanced in 1NP/1AP-treated cells, reflecting

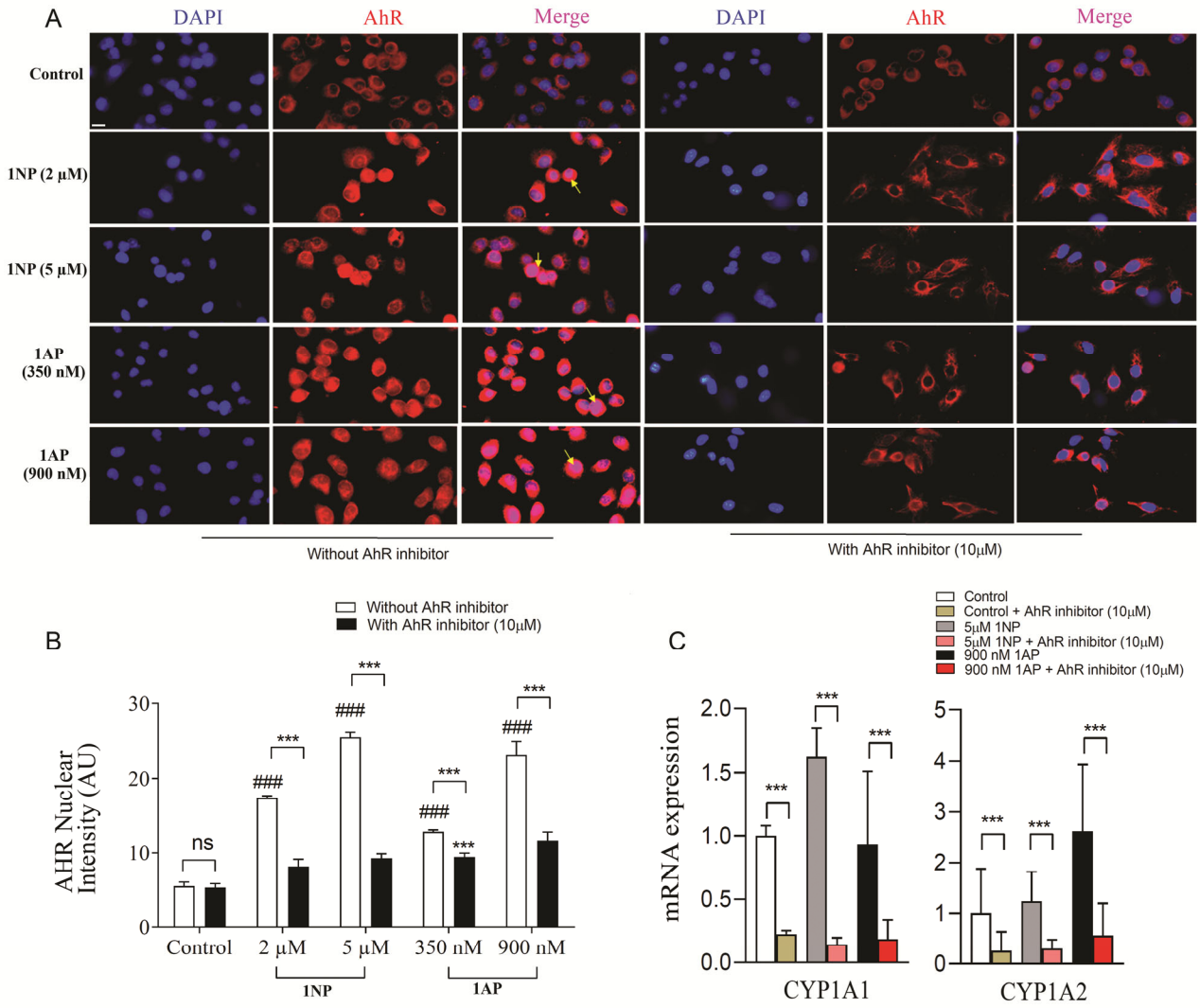

Fig. 4 — Effect of AhR inhibition on nuclear translocation and CYP gene expression in A549 cells. (A) Representative immunofluorescence images of A549 cells treated with 1NP and 1AP for 24 h in the presence or absence of an AhR inhibitor. Cells were stained with an anti-AhR antibody (red) and counterstained with DAPI for nuclei (blue). Yellow arrows indicate nuclear translocation of AhR (magenta signal). (B) Quantification of AhR nuclear signal intensity was performed using ImageJ software. > 50 cells were analysed per condition to ensure statistical robustness. (C) Relative mRNA expression levels of CYP1A1 and CYP1A2 were determined by qRT-PCR in A549 cells treated with 1NP or 1AP, with or without AhR inhibition. Data show fold changes compared with untreated controls. [Data are represented as Mean ± SD, ns = non-significant, ### or *** *P*-value <0.0001, SD = standard deviation: scale bar, 20 µm. (n=3)]

increased cell migration. Whereas co-treatment with an AhR inhibitor suppressed this effect, preventing scratch closure. The percentages of the scratch closing areas were evaluated, and quantitative analysis further demonstrated that the % scratch closing area significantly increased after 1NP/1AP treatment. As anticipated, scratch treated with 1NP/1AP in combination with an AhR inhibitor showed decreased percentages of scratch closing area (P<0.0001) (Fig. 7A & B). This concludes that the AhR activity is required for the migration of A549 cells in response to 1NP/1AP exposure.

A spheroid is a three-dimensional (3D) *in vitro* tumor model that mimics an *in vivo* environment. To assess the growth of 3D spheroids, A549 cells were exposed to 1NP/1AP with or without an AhR inhibitor by culturing them on an 8-well chamber slide. Cells treated with 1NP/1AP formed larger spheroids (P<0.0001) than the control, reflecting enhanced tumor-like growth (Fig. 8A & B), while spheroids derived from cells co-treated with 1NP/1AP and an AhR inhibitor were smaller, even smaller than those of the control. These findings confirm that AhR

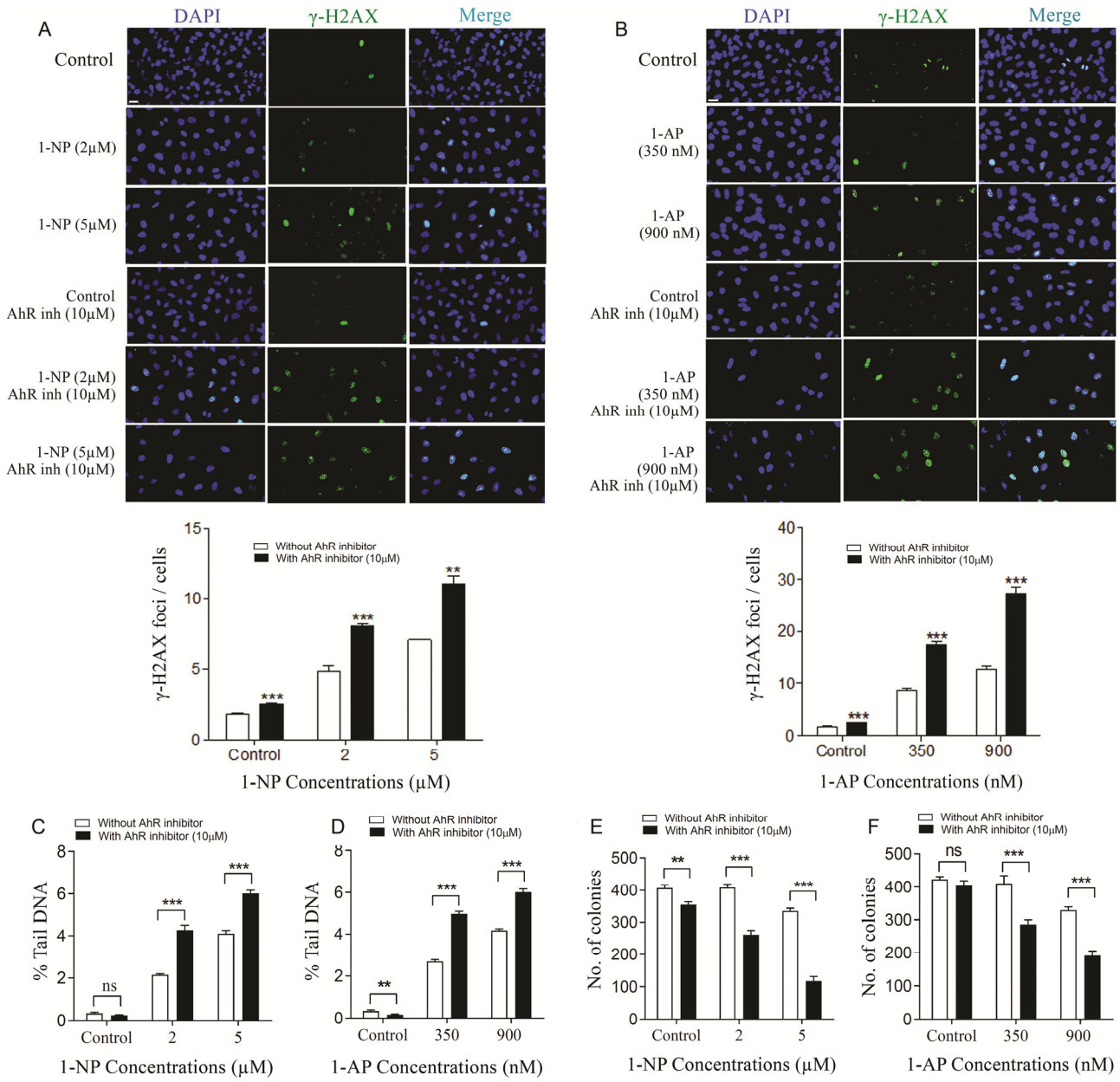

Fig. 5 — Effect of AhR inhibition on DNA damage and clonogenic survival in A549 cells. (A & B) Representative images (upper panels) and quantification (lower panels) of γ-H2AX foci per cell in A549 cells treated with 1NP and 1AP in the presence or absence of an AhR inhibitor. Scale bar: 10 μm. (C & D) Quantification of comet assay parameters in A549 cells treated with 1NP or 1AP under the same conditions (n = 3). (E & F) Quantification of colony-forming assay for A549 cells treated with 1NP or 1AP in the presence of an AhR inhibitor after 7 days (n = 3). ns = non-significant, ** *P*-value < 0.001, *** *P*-value < 0.0001, SD = standard deviation: scale bar, 10 μm.

activity is essential for the 3D tumor spheroid growth of A549 cells exposed to 1NP/1AP (Fig. 8A & B).

Discussion

Lung cancer globally accounts for 73.2% of cancer-related mortality. Asia has the highest burden of LC, representing 63.1% of cases and 62.9% of deaths, followed by Europe and North America[4,28]. The primary cause of LC is smoking, but poor air quality, particularly from vehicular emissions, also contributes significantly to the progression of the cancer. The association between DE and LC involves complex mechanisms that are not yet fully understood. Urinary 1AP has been used as a surrogate marker for evaluating DE exposure[29,30]. Recently, the conversion of 1NP to 1AP in LC cells was identified,

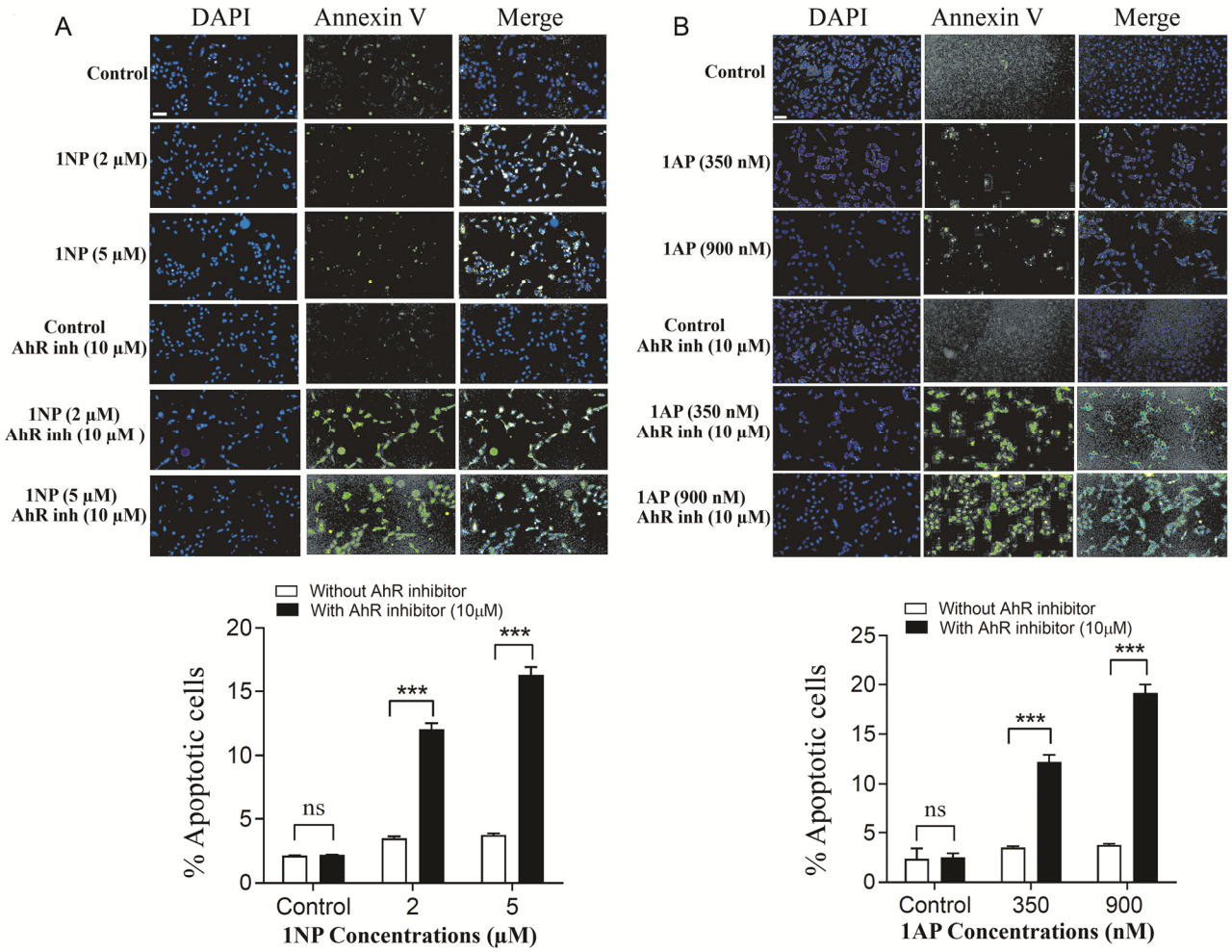

Fig. 6 — Effect of AhR inhibition on apoptosis in A549 cells. Representative images (left) of A549 cells treated with (A) 1NP and (B) 1AP in the presence of an AhR inhibitor for 24 hours, Annexin-V staining (green) to detect apoptotic cells. DAPI (blue) used for nuclear staining. Apoptotic cells in merge images (cyan) were quantified using ImageJ software. Quantification (right) shows the percentage of apoptotic cells treated with (A) 1NP and (B) 1AP in the presence of an AhR inhibitor (n = 3).ns = non-significant, *** *P*-value <0.0001, SD = standard deviation: scale bar, 10 µm.

but its impact on carcinogenesis remains unclear [9]. To address this, we investigated the toxicological effects of 1NP and its metabolite 1AP on A549 cells, focusing on (i) 1NP/1AP exposure induced ROS, DNA damage, and AhR activation in A549 cells. (ii) AhR activation is required for cell survival and carcinogenesis of A549 cells exposed to 1NP/1AP. (iii) AhR inhibitor-induced apoptosis, reduced cell migration, colony formation, and spheroid growth, and alleviated carcinogenesis induced by nitro-PAHs

In this study, we confirmed that exposure to 1NP/1AP causes ROS generation and DNA damage in A549 cells. These results were aligned with previous findings that 1NP induced oxidative stress in the human body[31]. Additionally, we reinforced the role of ROS in DNA damage, where the ROS level and DNA damage with NAC were observed to be reduced. However, if the damage is extensive or the repair mechanisms fail, it can lead to apoptosis or, conversely, uncontrolled cell proliferation and aggressive cancer development.

This study showed, despite the significant DNA damage caused by 1NP/1AP, no change in colony formation or spheroid size was observed (Fig. 3 & Fig. 5), suggesting that the cell survival mechanism may activated to detour the DNA damage response (DDR), In malignant cells, suppression of the DDR promotes survival and proliferation despite DNA damage by-passing cell cycle checkpoints, altered DDR protein expression, epigenetic changes, and activation of survival pathways[32,33].

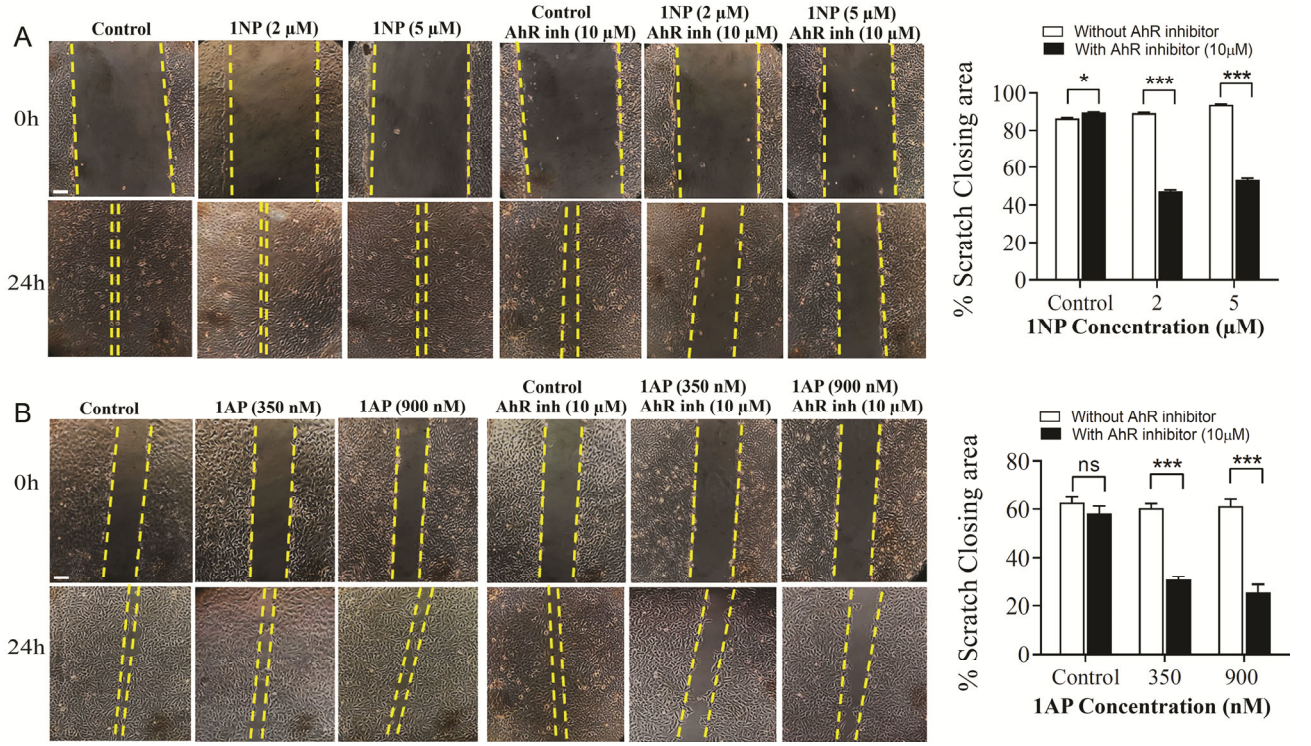

Fig. 7 — Effect of AhR inhibition on A549 cell migration. Representative images (left) and quantification (right) of the scratch wound-healing assay. Migration was assessed at 0 h and 24 h, and cell motility was evaluated as the percentage of scratch closure in A549 cells treated with (A) 1NP and (B) 1AP in the presence of an AhR inhibitor.ns = non-significant, * *P*-value < 0.05, *** *P*-value < 0.0001, SD = standard deviation. Scale bar, 50 µm. (n=3)

The ability of AhR to regulate both xenobiotic metabolism and DDR repair mechanisms place it at the centre of carcinogenesis induced by DE components[34,35]. Nuclear translocation of AhR induced by 1NP promotes *CYP1A1* gene expression, while 1AP promotes *CYP1A2* gene expression. This similar expression pattern for 1AP was consistent with the prior work in rat kidney cells reported by Miao *et al.*[36]. The structural characteristics of the metabolites, tissue-specific expression patterns, and various regulatory factors may influence such specific induction of these cytochrome P450 enzymes. Importantly, our data extend prior reports by Dittmann *et al.*[37] showed that in response to DNA damage by ionising radiation, AhR translocate into the nucleus and promotes DNA repair, suggesting that AhR activation may be involved in DNA repair.

Here, inhibiting AhR activity increased DNA damage and apoptosis in A549 cells, consistent with the studies showing that, in cancer, the AhR suppresses apoptosis, contrasting its role in normal cells. Inhibition of AhR has increased tumor cell susceptibility to chemotherapeutic agents[38]. In addition, Tetrachlorodibenzo-p-dioxin induced AhR activation, which inhibits apoptosis in lymphoma cells both *in vitro* and *in vivo* by inducing cyclooxygenase-2 (COX-2) and dysregulating Bcl-2 and UVB-irradiated keratinocytes, further supporting its anti-apoptotic role[39,40].

The present study also highlights the significant role of 1NP/1AP in promoting migration through AhR activation. Our findings, supported by the recent reports, demonstrated that AhR activation plays a central role in increased aggressiveness and tumor-cell migration in lung cancer cell lines exposed to kynurenine and benzo(a)pyrene [41].

The 3D spheroids provide a more physiologically relevant tumor model than 2D monolayers for *in vitro* environmental toxicant screening applications[42]. A549 cells were extensively used and studied for a 3D lung tumor model for screening inhibitors. We observed reduced spheroid size of A549 cells exposed to 1NP/1AP with AhR inhibitor. Notably, the study reported by Kim *et al.*[43] showed an elevated AhR expression in human LC. AhR may be involved in increased cancer aggression, as evidenced by the positive correlation seen between increased nuclear localisation of AhR in lung adenocarcinoma and lung squamous carcinoma and higher tumor grade. This is

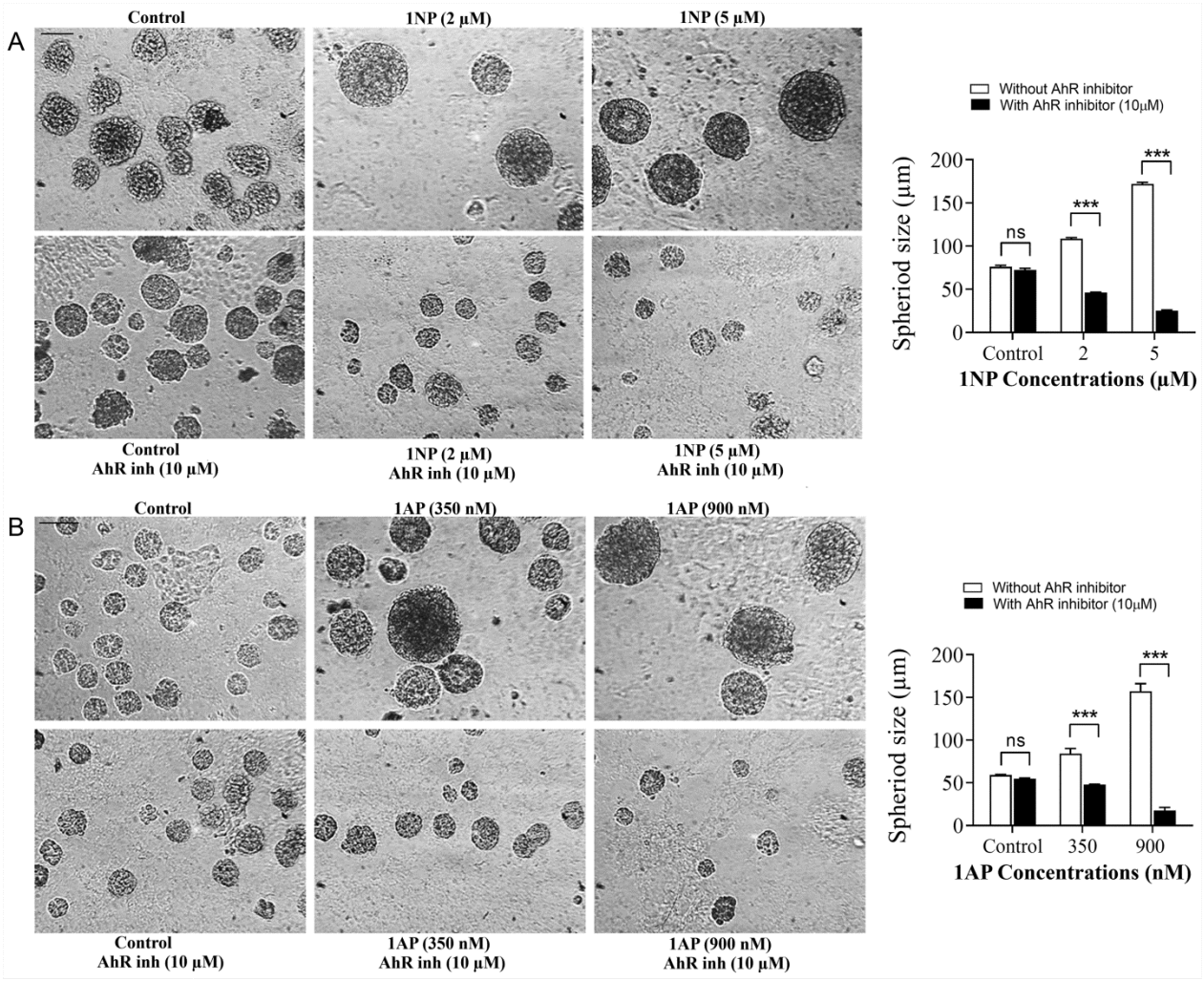

Fig. 8 — Effect of AhR inhibition on 3D spheroid growth in A549 cells. Representative images (left) and quantification (right) of 3D spheroids formed by A549 cells treated with (A) 1NP and (B) 1AP in the presence of an AhR inhibitor for 10 days. Quantitative analysis revealed a significant reduction in spheroid size under AhR inhibition (n = 3).ns = non-significant, *** *P*-value <0.0001, SD = standard deviation. Scale bar, 50 μm.

in line with our findings that AhR promotes A549 cell migration and 3D spheroid growth.

The broader implications of our study are twofold. First, our study suggests that AhR plays pleiotropic roles beyond xenobiotic metabolism, particularly under genotoxic stress. AhR serves as a central regulator of cancer cell survival under genotoxic stress caused by nitro-PAHs. Second, the results underscore the relevance of environmental pollutants such as 1NP/1AP in promoting tumor aggressiveness via AhR activation, suggesting that targeting AhR may represent a therapeutic strategy for lung cancer. From a methodological perspective, our use of 3D spheroids demonstrates their utility as a physiologically relevant model for environmental toxicology screening.

Nevertheless, this study has several limitations. First, it only examined the direct impact of 1NP/1AP on the survival of A549 cells, based on the hypothesis that AhR activation may regulate DNA damage repair caused by exposure to 1NP/1AP. However, this hypothesis requires further validation through *in vivo* studies. Second, the doses of 1NP/1AP used in this study were relatively high. In reality, the concentration of 1-NP in the atmosphere ranges from approximately 7–52 ng/m^3[29]. Future studies should examine chronic low-dose exposure and assess the long-term consequences for lung carcinogenesis.

Conclusion

This study demonstrates that nitro-PAHs from DE (1NP/1AP) induce genomic instability and regulate

AhR activation, which facilitates LC cell survival. The results of our study revealed that 1NP/1AP induced genomic instability and subsequent AhR activation in A549 cells. AhR activation was found to be a prerequisite for A549 cell survival, migration, and 3D spheroid formation, underscoring its role in lung cancer progression. To the best of our knowledge, this is the first evidence linking AhR activation to DNA repair-mediated survival of lung cancer under 1NP/1AP exposure. Importantly, inhibition of AhR exacerbated DNA damage and induced apoptosis, thereby suppressing cancer-promoting features, highlighting AhR as a promising therapeutic avenue for controlling LC and metastasis exposure to environmental 1NP/1AP. However, this study provides a foundation for future investigations into the mechanisms by which DNA repair mediates protective effects.

Acknowledgment

Ankita Bagde expresses gratitude for a fellowship from the University Grant Commission (UGC). Dr Atul Katarkar is thankful for the DBT-Ramalingaswami re-entry fellowship (Ref. No. BT/RLF/Re-entry/14/2021). KRC No.: CSIRNEERI/KRC/2025/ MARCH/WCTA/1

Conflict of interest

The authors declare no conflict of interest

References

1 World Cancer Research Fund International (2024) Lung cancer statistics. Available at: https://www.wcrf.org (Accessed: 5 February 2026). https://www.wcrf.org/ preventing-cancer/cancer-statistics/lung-cancer-statistics/page/157/?utm_source=chatgpt.com

2 Turner MC, Andersen ZJ, Baccarelli A, Diver WR, Gapstur SM, Pope III CA, Prada D, Samet J, Thurston G & Cohen A. Outdoor air pollution and cancer: An overview of the current evidence and public health recommendations. *CA Cancer J Clin,* 70 (2020) 460.

3 Sicard P, Khaniabadi YO, Perez S, Gualtieri M & De Marco A. Effect of O 3, PM 10 and PM 2.5 on cardiovascular and respiratory diseases in cities of France, Iran and Italy. *Environ. Sci. Pollut. Res,* 26 (2019) 32645.

4 Ferlay J, Ervik M, Lam F, Laversanne M, Colombet M, Mery L, Piñeros M, Znaor A, Soerjomataram I & Bray F. Global Cancer Observatory: Cancer Today (version 1.1). *Lyon, France: International Agency for Research on Cancer (*2024).

5 Gao R, Li D, Yun Y & Sang N. Dysfunction of the Hippo-Yap Pathway Drives Lung Cancer Metastasis Induced by 1-Nitropyrene through Adhesion Molecular Activation. *Environ. Sci. Technol. Lett,* 6 (2019) 270.

6 Libalova H, Zavodna T, Margaryan H, Elzeinova F, Milcova A, Vrbova K, Barosova H, Cervena T, Topinka J & Rössner P. Differential DNA damage response and cell fate in human lung cells after exposure to genotoxic compounds. *Toxicol. In Vitro*, 94 (2024)105710

7 Suresh A, Soman V, KR A, AR & Rahman KH. Sources, toxicity, fate and transport of polyaromatic hydrocarbons (PAHs) in the aquatic environment: A Review. *Environ. Forensics,* 26 (2025) 35.

8 Sola MCR, Santos AG, Martinez ST, Nascimento MM, da Rocha GO & de Andrade JB. Occurrence of 3-nitrobenzanthrone and other powerful mutagenic polycyclic aromatic compounds in living organisms: polychaetes. *Sci. Rep*,10 (2020) 3465.

9 Su AL & Penning TM. Role of Human Aldo-Keto Reductases and Nuclear Factor Erythroid 2-Related Factor 2 in the Metabolic Activation of 1-Nitropyrene via Nitroreduction in Human Lung Cells. *Chem. Res. Toxicol,*36 (2023) 270

10 Holme JA, Vondráček J, Machala M, Lagadic-Gossmann D, Vogel CF, Le Ferrec E, Sparfel L & Øvrevik J. Lung cancer associated with combustion particles and fine particulate matter (PM2. 5)-The roles of polycyclic aromatic hydrocarbons (PAHs) and the aryl hydrocarbon receptor (AhR). *Biochem. Pharmacol,216* (2023)115801.

11 Larigot L, Juricek L, Dairou J & Coumoul X. AhR signaling pathways and regulatory functions. *Biochim. Open,*7 (2018) 9.

12 Wang M, Luo N, Gao Y, Li G & An T. Pyrene and its derivatives increase lung adverse effects by activating aryl hydrocarbon receptor transcription. *STOTEN,* 916 (2024) 170030.

13 Kumar P, Nagarajan A & Uchil PD. Analysis of cell viability by the MTT assay. *Cold Spring Harb. Protoc*, (2018).

14 Olive PL & Banáth JP. The comet assay: a method to measure DNA damage in individual cells. *Nat. Protoc*, 1 (2006) 23.

15 Katarkar A, Mukherjee S, Khan MH, Ray JG & Chaudhuri K. Comparative evaluation of genotoxicity by micronucleus assay in the buccal mucosa over comet assay in peripheral blood in oral precancer and cancer patients. *Mutagenesis*, 29 (2014) 325.

16 Fu L, Zhao H, Xiang Y, Xiang HX, Hu B, Tan ZX, Lu X, Gao L, Wang B, Wang H & Zhang C. Reactive oxygen species-evoked endoplasmic reticulum stress mediates 1-nitropyrene-induced epithelial-mesenchymal transition and pulmonary fibrosis. *Environ. Pollut,* 283 (2021) 117134.

17 Roy A, Ahir M, Bhattacharya S, Parida PK, Adhikary A, Jana K & Ray M. Induction of mitochondrial apoptotic pathway in triple negative breast carcinoma cells by methylglyoxal via generation of reactive oxygen species. *Mol. Carcinog,* 56 (2017) 2086.

18 Franken NAP, Rodermond HM, Stap J, Haveman J & van Bree C. Clonogenic assay of cells in vitro. *Nat. Protoc*,1(2006) 2315.

19 Pahlevan Kakhki M. TRIzol-based RNA extraction: a reliable method for gene expression studies. *JSIRI*, 25 (2014) 13.

20 Chang TKH, Chen J, Pillay V, Ho JY & Bandiera SM. Real-time polymerase chain reaction analysis of CYP1B1 gene expression in human liver. *Tox. Sci,* 71 (2003) 11.

21 Naqvi SMA, Islam SN, Kumar A, Patil CR, Kumar A & Ahmad A. Enhanced anti-cancer potency of sustainably synthesized anisotropic silver nanoparticles as compared

with L-asparaginase. *Int J Biol Macromol,* 263 (2024) 130238.
22 Wang B, Xu S, Lu X, Ma L, Gao L, Zhang SY, Li R, Fu L, Wang H, Sun GP & Xu DX. Reactive oxygen species-mediated cellular genotoxic stress is involved in 1-nitropyrene-induced trophoblast cycle arrest and fetal growth restriction. *Environ. Pollut,* 260 (2020) 113984.
23 Aslan M, Hsu EC, Liu S & Stoyanova T. Quantifying the invasion and migration ability of cancer cells with a 3D Matrigel drop invasion assay. *Biol. methods protoc*, 6 (2021) 014.
24. Bresciani G, Hofland LJ, Dogan F, Giamas G, Gagliano T & Zatelli MC. Evaluation of Spheroid 3D Culture Methods to Study a Pancreatic Neuroendocrine Neoplasm Cell Line. *Front. Endocrinol*, 10 (2019) 682.
25 Denison MS & Nagy SR. Activation of the aryl hydrocarbon receptor by structurally diverse exogenous and endogenous chemicals. *Annu. Rev. Pharmacol. Toxicol,* 43 (2003) 309.
26 Gutiérrez-Vázquez C & Quintana FJ. Regulation of the immune response by the aryl hydrocarbon receptor. *Immunity*, 48 (2018) 19.
27 Puga A, Xia Y & Elferink C. Role of the aryl hydrocarbon receptor in cell cycle regulation. *Chem Biol Interact*, 141 (2002) 117.
28 Zhou J, Xu Y, Liu J, Feng L, Yu J & Chen D. Global burden of lung cancer in 2022 and projections to 2050: Incidence and mortality estimates from GLOBOCAN. *Cancer Epidemiol,* 93 (2024) 102693.
29 Wadikar DL, Farooqui MO, Middey A, Bafana A, Pakade Y, Naoghare P, Vanisree AJ, Kannan K & Sivanesan S. Assessment of occupational exposure to diesel particulate matter through evaluation of 1-nitropyrene and 1-aminopyrene in surface coal miners, India. *Environ. Monit.Assess,* 193 (2021) 342.
30 Ochirpurev B, Eom SY, Toriba A, Kim YD & Kim H. Urinary 1-aminopyrene level in Koreans as a biomarker for the amount of exposure to atmospheric 1-nitropyrene. *Toxicol. Res,* 38 (2022) 45.
31 Choi SH, Ochirpurev B, Toriba A, Won JU & Kim H. Exposure to Benzo [a] pyrene and 1-Nitropyrene in Particulate Matter Increases Oxidative Stress in the Human Body. *Toxics*, 11 (2023) 797.
32 Glaviano A, Foo AS, Lam HY, Yap KC, Jacot W, Jones RH, Eng H, Nair MG, Makvandi P, Geoerger B & Kulke MH. PI3K/AKT/mTOR signaling transduction pathway and targeted therapies in cancer. *Mol.Cancer,* 22 (2023) 138.
33 Bartek J & Lukas J. Chk1 and Chk2 kinases in checkpoint control and cancer. *Cancer cell*, 3 (2003) 421.
34 Vaddavalli PL & Schumacher B. The p53 network: cellular and systemic DNA damage responses in cancer and aging. *TIG*, 38 (2022) 598.
35 O'Donovan PJ & Livingston DM. BRCA1 and BRCA2: breast/ovarian cancer susceptibility gene products and participants in DNA double-strand break repair. *Carcinogenesis*, 31 (2010) 961.
36 Miao H, Cao G, Wu XQ, Chen YY, Chen DQ, Chen L, Vaziri ND, Feng YL, Su W, Gao Y & Zhuang S. Identification of endogenous 1-aminopyrene as a novel mediator of progressive chronic kidney disease via aryl hydrocarbon receptor activation. *Br. J. Pharmacol,* 177 (2020) 3415.
37 Dittmann KH, Rothmund MC, Paasch A, Mayer C, Fehrenbacher B, Schaller M, Frauenstein K, Fritsche E, Haarmann-Stemmann T, Braeuning A & Rodemann HP. The nuclear aryl hydocarbon receptor is involved in regulation of DNA repair and cell survival following treatment with ionizing radiation. *Toxicol. Lett,* 240 (2016) 122.
38 Stanford EA, Ramirez-Cardenas A, Wang Z, Novikov O, Abalkhail KA, Koutrakis P, Mizgerd JP, Genco CA, Kukuruzinska M, Monti S & Bais MV. Role for the aryl hydrocarbon receptor and diverse ligands in oral squamous cell carcinoma migration and tumorigenesis. *Mol Cancer Res*, 14 (2016) 696.
39 Vogel CFA, Sciullo E & Matsumura F. Activation of inflammatory mediators and potential role of ah-receptor ligands in foam cell formation. *Cardiovasc. Toxicol,* 4 (2004) 363.
40 Pollet M, Shaik S, Mescher M, Frauenstein K, Tigges J, Braun SA, Sondenheimer K, Kaveh M, Bruhs A, Meller S & Homey B. The AHR represses nucleotide excision repair and apoptosis and contributes to UV-induced skin carcinogenesis. *Cell Death Differ,* 25 (2018) 1823.
41 Attafi IM, Bakheet SA & Korashy HM. The role of NF-κB and AhR transcription factors in lead-induced lung toxicity in human lung cancer A549 cells. *Toxicol. Mech. Methods,* 30 (2020) 197.
42 Juarez-Moreno K, Chávez-García D, Hirata G & Vazquez-Duhalt R. Monolayer (2D) or spheroids (3D) cell cultures for nanotoxicological studies? Comparison of cytotoxicity and cell internalization of nanoparticles. *Toxicol In Vitro,* 85 (2022) 105461.
43 Kim DK, Lee CY, Han YJ, Park SY, Han H, Na K, Kim MH, Yang SM, Baek S, Kim Y & Hwang JY. Exploring aryl hydrocarbon receptor expression and distribution in the tumor microenvironment, with a focus on immune cells, in various solid cancer types. *Front. Immunol,* 15 (2024) 1330228.